JCTC Journal of Chemical Theory and Computation

Article

pubs.acs.org/JCTC

# Nonvariational Orbital Optimization Techniques for the AP1roG Wave Function

Katharina Boguslawski,*[,†] Paweł Tecmer,[†] Patrick Bultinck,[‡] Stijn De Baerdemacker,[¶] Dimitri Van Neck,[¶] and Paul W. Ayers*[,†]

[†]Department of Chemistry and Chemical Biology, McMaster University, 1280 Main Street West, Hamilton, L8S 4M1 Ontario, Canada

[‡]Department of Inorganic and Physical Chemistry, Ghent University, Krijgslaan 281 (S3), 9000 Gent, East Flanders, Belgium

[¶]Center for Molecular Modelling, Ghent University, Technologiepark 903, 9052 Gent, East Flanders, Belgium

**ABSTRACT:** We introduce new nonvariational orbital optimization schemes for the antisymmetric product of one-reference orbital geminal (AP1roG) wave function (also known as pair-coupled cluster doubles) that are extensions to our recently proposed projected seniority-two (PS2-AP1roG) orbital optimization method [*J. Chem. Phys.* **2014**, *140*, 214114)]. These approaches represent less stringent approximations to the PS2-AP1roG ansatz and prove to be more robust approximations to the variational orbital optimization scheme than PS2-AP1roG. The performance of the proposed orbital optimization techniques is illustrated for a number of well-known multireference problems: the insertion of Be into $H_2$, the automerization process of cyclobutadiene, the stability of the monocyclic form of pyridyne, and the aromatic stability of benzene.

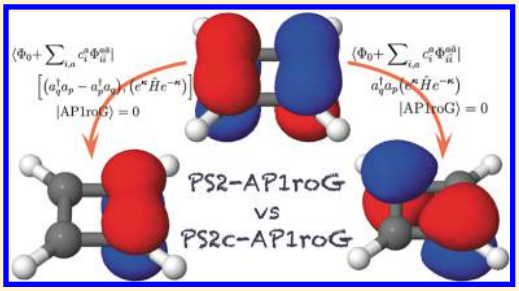


## 1. INTRODUCTION

In nonrelativistic quantum theory, the exact solution of the electronic Schrödinger equation for a given atomic basis set is provided by the full configuration interaction (FCI) wave function. However, the factorial scaling of FCI limits its applicability to only small systems or basis sets. This deficiency leads to the development of various computationally more convenient approaches for describing quantum many-body systems in condensed-matter physics and quantum chemistry.[1,2]

One rapidly developing field of research represents coupled cluster (CC) theory. Although being originally introduced to study phenomena in nuclear physics,[3] the CC ansatz became a popular technique for modeling ground and excited electronic states of atoms and molecules.[4] In present-day quantum chemistry, CC is one of the most prevalent and reliable methods for treating weak (or dynamic) electron correlation.[5,6] The other popular wave function-based method for describing weak electron correlation is many-body perturbation theory (MBPT).[6] MBPT is computationally cheaper but in many cases less reliable than CC.

In contrast to weak electron correlation, electronic structure theory still seeks methods that can properly account for strong electron correlation effects but simultaneously do not sacrifice computational feasibility. One family of conventional quantum chemistry approaches suitable for strong electron correlation covers the multi-configurational self-consistent-field (MCSCF) methods.[7] Examples of MCSCF-type techniques are the complete-active-space (CAS) SCF,[8,9] the restrictive-active-space SCF,[10] and the generalized-active space SCF[11] approaches. Different methods to model the strong electron correlation problem also emerged within multireference CC theory,[12−15] different variants of CC approaches,[16−18] the density matrix renormalization group algorithm,[19−32] and the symmetry projected Hartree−Fock methods.[33,34]

A conceptually different way of describing strong electron correlation is to include electron correlation effects directly in the electronic wave function using two-electron functions, also called geminals. If geminals are restricted to be singlet (two-electron) functions, a pair-excitation function (in its natural form[35,36]) can be written as

$$\Psi_i^\dagger = \sum_{p=1}^{M_i} c_p^i a_p^\dagger a_{\bar{p}}^\dagger \tag{1}$$

with $a_p^\dagger$ and $a_{\bar{p}}^\dagger$ being the electron creation operators for spin-up ($p$) and spin-down electrons ($\bar{p}$) for orbital $p$, while ($c_p^i$) is the $P \times M$ geminal coefficient matrix that links the underlying one-particle functions (orbitals) with the two-particle functions $\Psi_i^\dagger$ (geminals). In eq 1, each geminal $\Psi_i^\dagger$ is constructed from orbitals confined to (possibly disjoint) orbital subspaces $M_i$. The geminal-based wave function has then the form

$$|\text{Geminal}\rangle = \prod_i^P \Psi_i^\dagger |\Phi_0\rangle \tag{2}$$

where $P$ is the number of electron pairs, and $|\Phi_0\rangle$ is the vacuum state with respect to the creation of geminals.

**Received:** August 21, 2014
**Published:** September 22, 2014

   dx.doi.org/10.1021/ct500759q | *J. Chem. Theory Comput.* 2014, 10, 4873−4882

If we impose specific restrictions on the subspaces $M_i$ and on $\{c_p^i\}$, we can deduce different geminal models. Examples thereof are generalized-valence-bond perfect-pairing[37−39] (GVB-PP), the antisymmetric product of strongly orthogonal geminals[40−44] (APSG), the particle-number projected Hartree−Fock−Bogoliubov ansatz,[45] or the antisymmetric product of interacting geminals[35,36,45−56] (APIG). However, these method-dependent constraints on $M_i$ and $\{c_p^i\}$ are either too stringent and thus neglect a large portion of electron correlation effects (such as GVB-PP, APSG) or are computationally intractable for large quantum many-body systems (such as APIG) and thus limited to very small systems.

We can account for correlation between all orbital pairs and simultaneously guarantee computational feasibility if we impose a *special* structure on the geminal coefficient matrix. By doing so, the permanent of any relevant $P \times P$ submatrix of the $P \times M$ coefficient matrix $(c_p^i)$ can be evaluated efficiently in polynomial time. One possible choice is to restrict each geminal to contain one unique occupied orbital (of some reference determinant $|\Phi_0\rangle$), while $\{c_p^i\}$ of the unoccupied orbitals (of some reference determinant $|\Phi_0\rangle$) are allowed to vary freely.[57,58] This ansatz has been introduced by some of us in ref 57 as the antisymmetric product of 1-reference orbital geminal (AP1roG). Specifically, the AP1roG wave function can be written as a general pair-coupled-cluster-doubles wave function in terms of one-particle functions (see, e.g., ref 18)

$$|\mathrm{AP1roG}\rangle = \exp\Big(\sum_{i=1}^{P}\sum_{a=P+1}^{K} c_i^a a_a^\dagger a_{\bar{a}}^\dagger a_{\bar{i}} a_i\Big)|\Phi_0\rangle \tag{3}$$

where $a_p$ and $a_{\bar{p}}$ are the electron annihilation operators for spin-up $(p)$ and spin-down electrons $(\bar{p})$, and $|\Phi_0\rangle$ is some independent-particle wave function (usually the Hartree−Fock (HF) determinant). The exponential ansatz of AP1roG ensures, by construction, size-extensivity, while size-consistency can be recovered by optimizing the one-particle basis functions given that the optimized orbitals are symmetry-broken (i.e., localized).[59]

This work is organized as follows. In section 2, we will discuss different algorithms to optimize the orbitals within the AP1roG framework. Their performance is compared by studying some well-known multireference problems of quantum chemistry: the Be−$H_2$ insertion problem, the automerization of cyclobutadiene, the bicyclic and monocyclic isomers of pyridyne, and the aromatic stability of benzene. Computational details are presented in section 3.

## 2. ORBITAL-OPTIMIZATION PROCEDURES

A standard procedure to optimize the one-particle basis functions is to use the variational principle. The optimal set of one-particle basis functions is then obtained by minimizing an energy Lagrangian.[2] Variational approaches are most commonly used in orbital-optimization algorithms of electronic structure theory. Yet, different techniques that do not exploit the variational principle have been introduced as well, e.g. Brueckner coupled cluster theory.[60]

We have recently presented an orbital-optimization scheme for AP1roG that does not rely on the variational principle.[61] Our approach is based on the assumption that the seniority-zero-plus-two ($\Omega$ = 0, 2) sectors and the seniority-zero ($\Omega$ = 0) sector can be decoupled (see refs 62−65 for further details on the seniority number that is defined as the number of unpaired electrons in a Slater determinant). The optimal set of orbitals is chosen such that the decoupling condition is satisfied. In the following, we will shortly discuss the relation between orbital optimization and decoupling of the $\Omega$ = 0, 2 and $\Omega$ = 0 sectors. For that purpose, let $\Psi_{oo}^{(0)}$ be a CI expansion comprising only closed-shell configurations, i.e., a seniority-zero wave function, constructed from a set of optimized orbitals. Further, consider $\Psi_{oo}^{(0,2)}$ to be CI expansion containing both closed-shell Slater determinants and Slater determinants with exactly two unpaired electrons, i.e., a CI expansion restricted to the seniority-zero-plus-two sectors, again with optimized orbitals. Assuming that the optimal seniority-zero-plus-two solution is very close to the optimal seniority-zero solution, one can write

$$\Psi_{oo}^{(0,2)} = \Psi_{oo}^{(0)} + \Psi_{oo}^{(2)} = \Big(1 + \sum_{p\neq q} t_{pq} a_p^\dagger a_q\Big)\Psi_{oo}^{(0)} \tag{4}$$

where $\{t_{pq}\}$ are some expansion coefficients. The seniority-zero-plus-two sectors and the seniority-zero sector can be decoupled if CI expansions restricted to the $\Omega$ = 0, 2 and $\Omega$ = 0 sector have the same energy expectation value. Thus, the following equation must hold

$$\langle\Psi_{oo}^{(0,2)}|\hat{H}|\Psi_{oo}^{(0,2)}\rangle - \langle\Psi_{oo}^{(0)}|\hat{H}|\Psi_{oo}^{(0)}\rangle = 0 \tag{5}$$

The above condition is satisfied to first order in $\{t_{pq}\}$ if $(t_{pq})$ is a skew-symmetric matrix.[2] In this case, the seniority-two contribution of $\Psi_{oo}^{(0,2)}$ (the second term on the right-hand side of eq 4) can be written as

$$\Psi_{oo}^{(2)} = \sum_{p>q} t_{pq}(a_p^\dagger a_q - a_q^\dagger a_p)\Psi_{oo}^{(0)} \tag{6}$$

Using the above equation, the decoupling condition eq 5 can be straightforwardly simplified. Keeping only terms up to first order in $\{t_{pq}\}$, we obtain the approximate decoupling condition

$$\langle\Psi_{oo}^{(2)}|\hat{H}|\Psi_{oo}^{(0)}\rangle + \langle\Psi_{oo}^{(0)}|\hat{H}|\Psi_{oo}^{(2)}\rangle + \mathrm{O}(t^2) = 0$$

Substituting eq 6 in the above equation, the approximate decoupling condition can be reformulated as

$$\langle\Psi_{oo}^{(0)}|[(a_q^\dagger a_p - a_p^\dagger a_q), \hat{H}]|\Psi_{oo}^{(0)}\rangle = 0 \;\forall\; p > q \tag{7}$$

which is equivalent to the generalized Brillouin theorem[66] of a seniority-zero wave function for the orbital parameters.[67,68] Thus, the decoupling of the seniority-zero-plus-two sectors and the seniority-zero sector is equivalent to satisfying the orbital-dependent part of the generalized Brillouin theorem of an $\Omega$ = 0 wave function to first order. In cases where higher order terms in $\{t_{pq}\}$ become important, the simplification of eq 5 to satisfy eq 7 is not valid and a seniority-zero-plus-two wave function will result in a lower energy expectation value than a CI expansion constrained to the seniority-zero sector.[63]

In the following, we will use eq 7 as a starting point to derive different approximate orbital-optimization schemes.

### 2.1. Projected-Seniority-Two Approximation Schemes.

Choosing the optimal set of orbitals such that eq 7 is satisfied scales factorially with system size. We can reduce the computational cost by making two assumptions as outlined in ref 57. First, we assume that the AP1roG model is a decent approximation to a seniority-zero wave function, i.e., $|\mathrm{AP1roG}\rangle \approx |\Psi^{(0)}\rangle$. The good performance of AP1roG in approximating the doubly occupied CI (DOCI) wave function (a wave function restricted to the seniority-zero sector) has been shown in many numerical examples.[57,59,61,69−71] Then, the rotated set of orbitals can be obtained by solving

$$\langle \mathrm{AP1roG}|[(a_q^\dagger a_p - a_p^\dagger a_q), \hat{H}]|\mathrm{AP1roG}\rangle = 0 \;\forall\; p > q \tag{8}$$

Yet, the cost of solving the above equation still grows factorially with system size, and we are compelled to make further simplifications for the sake of computational tractability. Our second, more pragmatic assumption is, therefore, to restrict the excitation manifold to all singly pair excited determinants with respect to the reference determinant $|\Phi_0\rangle$. Thereby, the optimal set of orbitals can be determined in a computationally efficient way. In doing so, eq 8 reduces to

$$\langle \Phi_0 + \sum_{i,a} c_i^a \Phi_{i\bar{i}}^{a\bar{a}} | [(a_q^\dagger a_p - a_p^\dagger a_q), (e^{\boldsymbol{\kappa}} \hat{H} e^{-\boldsymbol{\kappa}})] | \mathrm{AP1roG}\rangle = 0 \;\forall\; p > q \tag{9}$$

where we have written the Hamiltonian explicitly in terms of the rotated basis, and $\boldsymbol{\kappa}$ is the generator of orbital rotations

$$\boldsymbol{\kappa} = \sum_{p>q} \kappa_{pq} (a_p^\dagger a_q - a_q^\dagger a_p) \tag{10}$$

and accounts for all nonredundant orbital rotations within the occupied-occupied, occupied-virtual, and virtual−virtual orbital blocks.[59] Eq 9 represents our starting point for different orbital-optimization procedures that aim at decoupling the seniority-zero and seniority-zero-plus-two sectors.

In our first approach, no further approximations are made, and the $\{\kappa_{pq}\}$ are optimized such that eq 9 is fulfilled. Since the action of $a_p^\dagger a_q$ on the bra-state (or equivalently on the ket-state) of eq 9 generates a seniority-two wave function, the optimized set of orbitals is obtained by requiring that the projection of the seniority-two sector on the AP1roG wave function vanishes, i.e., the Hamiltonian does not connect the seniority-two and seniority-zero sectors in the case of an optimal basis. Thus, we will call eq 9 the projected-seniority-two condition using the commutator formulation (PS2c) and the left-hand side of eq 9 the PS2c orbital gradient. The PS2c method bears similarity to the variational orbital optimization scheme.[59] In section 2.2, we will compare the working equations of the PS2c approximation to those used in variational orbital optimization.

In our second orbital-optimization procedure, we impose the stronger condition that each term of the commutator vanishes separately

$$\langle \Phi_0 + \sum_{i,a} c_i^a \Phi_{i\bar{i}}^{a\bar{a}} | (a_q^\dagger a_p - a_p^\dagger a_q)(e^{\boldsymbol{\kappa}} \hat{H} e^{-\boldsymbol{\kappa}}) | \mathrm{AP1roG}\rangle = 0 \;\forall\; p > q \tag{11}$$

Note that the above equation is still antisymmetric in its indices $p,q$. We will refer to eq 11 as the antisymmetric PS2 condition (PS2a) and the left-hand side of eq 11 as the PS2a orbital gradient.

In our most stringent approximation, we require that the first term of eq 11 equals zero individually, and the projected-seniority-two condition simplifies to

$$\langle \Phi_0 + \sum_{i,a} c_i^a \Phi_{i\bar{i}}^{a\bar{a}} | a_q^\dagger a_p (e^{\boldsymbol{\kappa}} \hat{H} e^{-\boldsymbol{\kappa}}) | \mathrm{AP1roG}\rangle = 0 \;\forall\; p > q \tag{12}$$

This choice was motivated by the analogy to the Brillouin theorem of HF theory. Note that in the case of HF theory, the above relation is known as the Brillouin theorem for a closed-shell Slater determinant. The above equation has been introduced in ref 61 as the PS2 condition and its left-hand side as the PS2 orbital gradient. For both the PS2 and PS2a approximation, the $\{\kappa_{pq}\}$ are obtained by solving eqs 11 and 12, respectively.

**2.2. Comparison to Variational Orbital Optimization.** In variational orbital optimization (vOO), the orbitals are chosen to minimize the AP1roG energy functional subject to the constraint that the AP1roG coefficient equations are satisfied.[57] In intermediate normalization, the energy Lagrangian has thus the form

$$\mathcal{L} = \langle \Phi_0 | e^{\boldsymbol{\kappa}} \hat{H} e^{-\boldsymbol{\kappa}} | \mathrm{AP1roG}\rangle + \sum_{i,a} \lambda_i^a (\langle \Phi_{i\bar{i}}^{a\bar{a}} | e^{\boldsymbol{\kappa}} \hat{H} e^{-\boldsymbol{\kappa}} | \mathrm{AP1roG}\rangle - E c_i^a) \tag{13}$$

where $\{\lambda_i^a\}$ are the Lagrange multipliers. The requirement that the derivative of $\mathcal{L}$ with respect to the Lagrange multipliers $\{\lambda_i^a\}$ is stationary results in the standard set of equations for the geminal coefficients $\{c_i^a\}$

$$\frac{\partial \mathcal{L}}{\partial \lambda_i^a} = \langle \Phi_{i\bar{i}}^{a\bar{a}} | e^{\boldsymbol{\kappa}} \hat{H} e^{-\boldsymbol{\kappa}} | \mathrm{AP1roG}\rangle - E c_i^a = 0 \tag{14}$$

while the stationary requirement of $\mathcal{L}$ with respect to the geminal coefficients, $\frac{\partial \mathcal{L}}{\partial c_i^a} = 0$, leads to a set of equations for the Lagrange multipliers, analogous to the Λ-equations in CC theory

$$\frac{\partial \mathcal{L}}{\partial c_i^a} = \langle \Phi_0 | (e^{\boldsymbol{\kappa}} \hat{H} e^{-\boldsymbol{\kappa}}) a_a^\dagger a_{\bar{a}}^\dagger a_{\bar{i}} a_i | \mathrm{AP1roG}\rangle + \sum_{jb} \lambda_j^b \langle \Phi_{j\bar{j}}^{b\bar{b}} | (e^{\boldsymbol{\kappa}} \hat{H} e^{-\boldsymbol{\kappa}}) a_a^\dagger a_{\bar{a}}^\dagger a_{\bar{i}} a_i | \mathrm{AP1roG}\rangle - E \lambda_i^a - \langle i\bar{i}|a\bar{a}\rangle \sum_{jb} \lambda_j^b c_j^b = 0 \tag{15}$$

The variational orbital gradient is the derivative of $\mathcal{L}$ with respect to the orbital rotation coefficients $\{\kappa_{pq}\}$

$$\frac{\partial \mathcal{L}}{\partial \kappa_{pq}} = \langle \Phi_0 + \sum_{i,a} \lambda_i^a \Phi_{i\bar{i}}^{a\bar{a}} | [(a_p^\dagger a_q - a_q^\dagger a_p), e^{\boldsymbol{\kappa}} \hat{H} e^{-\boldsymbol{\kappa}}] | \mathrm{AP1roG}\rangle - \langle \Phi_0 | [(a_p^\dagger a_q - a_q^\dagger a_p), e^{\boldsymbol{\kappa}} \hat{H} e^{-\boldsymbol{\kappa}})] | \mathrm{AP1roG}\rangle \sum_{ia} \lambda_i^a c_i^a \tag{16}$$

The set of eqs 14−16 can be considered as the generalized Brillouin theorem of vOO-AP1roG and bears close analogy to the generalized Brillouin theorem of orbital-optimized CC. Within the vOO-AP1roG approximation, $p,q$ run over all (occupied and virtual) orbital indices.[59] We should emphasize that, in the case of orbital-optimized AP1roG, the term variational only refers to the orbital rotation part of the wave function optimization. The optimal set of orbitals is obtained by minimizing the energy Lagrangian eq 13, while the geminal coefficients are obtained by solving the projected Schrödinger equation. Since this procedure of optimizing the orbitals is known as variational orbital optimization in CC theory, we will refer to the minimization of the energy Lagrangian as variational orbital optimization.

The variational orbital gradient and the PS2c orbital gradient (left-hand side of eq 9) are similar if $\lambda_i^a \approx c_i^a$ and if the second term of eq 16 is negligible. Thus, the vOO and PS2c schemes are expected to result in similar orbitals and ground-state energies for a system where strong electron correlation effects are moderate. Note, however, that all orbital optimization approaches have different equations for the orbital gradient and


dx.doi.org/10.1021/ct500759q | J. Chem. Theory Comput. 2014, 10, 4873−4882

cannot be zero at the same time. The general exception are two-electron systems where all methods are equivalent to FCI.

## 3. COMPUTATIONAL DETAILS

The full-CI, MP2, CASSCF, and NEVPT2 calculations were performed with the DALTON2013[72] software package. For cyclobutadiene, two different active spaces were chosen. In the minimal active space calculation, only the $\pi$- and $\pi^*$-orbitals were correlated, resulting in CAS(4,4)SCF. This minimal active space was further extended by including the 1*s* orbitals of the H atoms as well as the C 2*s* and one additional C 2*p* orbital per C atom leading to a CAS(20,16) active space. A full valence CASSCF calculation (CAS(20,20)SCF) was computationally not feasible, and the CAS(20,16) active space was chosen based on MP2 natural occupation numbers.

For the pyridyne molecule, a CAS(8,8)SCF was chosen in accordance with ref 73, where the three $\pi$- and $\pi^*$-orbitals and two nonbonding $\sigma$-orbitals were correlated.

All geminal calculations have been performed in a developer version of the HORTON[74] software package, where the PS2c and PS2a orbital-optimization schemes have been implemented. Specifically, we used a Newton−Raphson optimizer and a diagonal approximation of the Jacobian (containing terms at most linear in the geminal expansion coefficients) to obtain the rotated set of orbital expansion coefficients. All restricted AP1roG calculations (vOO, PS2a, PS2c, and PS2) were allowed to relaxed freely without any spatial symmetry constraints, i.e., no point group symmetry was imposed. As initial guess orbitals, (delocalized) canonical restricted Hartree−Fock orbitals were taken for cyclobutadiene, pyridyne, and benzene. For the $BeH_2$ molecule, the localized solutions of the neighboring points of the reaction coordinate were used as initial guess orbitals to overcome convergence difficulties encountered with canonical Hartree−Fock orbitals. In all geminal calculations all electrons and all orbitals were correlated; the corresponding active spaces are summarized in Table 1.

**Table 1. Size of the Active Spaces (Number of Electrons $N_e$ and Number of Orbitals $N_O$) in All Orbital-Optimized AP1roG Calculations**

| molecules | $N_e$ | $N_o$ |
|---|---|---|
| $BeH_2$ | 6 | 28 |
| cyclobutadiene | 28 | 72 |
| pyridyne | 40 | 123 |
| benzene | 42 | 138 |

**3.1. Basis Sets.** For Be, C, and N in $BeH_2$, pyridyne, and benzene, Dunning's cc-pCVDZ[75−77] basis set was used with the following contraction: $(10s5p1d) \rightarrow [4s3p1d]$. The cc-pVDZ[75] basis set was utilized for the H atoms in these systems (H: $(4s1p) \rightarrow [2s1p]$). For cyclobutadiene, Dunning's cc-pVDZ basis set was used for all atoms ((10s5p1d) → [4s3p1d]).

## 4. RESULTS AND DISCUSSION

**4.1. The Insertion of the Be Atom into the $H_2$ Molecule.** The theoretical modeling of the quasi-reaction path for the insertion of Be into $H_2$ (perpendicular $C_{2v}$ pathway) to form the linear H−Be−H molecule represents a challenging problem for single-reference methods.[14,34,78−87] To insert the Be atom into the $H_2$ molecule, the two H atoms need to be pulled apart which leads to two nearly degenerate electronic configurations ($1\sigma_u^2$ and $1\sigma_g^2$) for stretched internuclear H−H separations. Furthermore, the quasi-degeneracy of the 2*s* and 2*p* orbitals in the Be atom gives further rise to two important configurations ($1s^2 2s^2$ and the $1s^2 2p^2$).

In the linear coordination pathway proposed by Purvis,[78] the two hydrogen atoms move along a reaction pathway (here

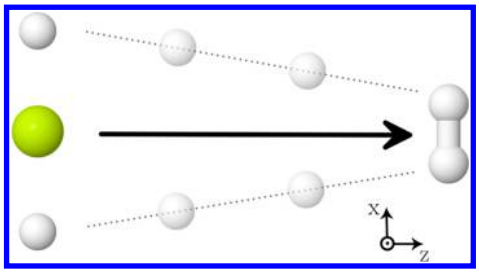


**Figure 1.** Schematic representation of the $BeH_2 \rightarrow Be+H_2$ reaction pathway.

along the *z*-axis as shown in Figure 1) described by the following coordinate function

$$r_z(x) = \pm(2.54 - 0.46x) \quad (17)$$

while the beryllium atom is located in the origin of the coordinate frame. The transition state occurs at around $r_z(x) = 2.75$ bohr. At equilibrium geometry, the $(1a_1)^2(2a_1)^2(1b_2)^2$ electronic configuration represents the dominant contribution to the wave function. On the other hand, there are two leading quasi-degenerate electronic configurations $((1a_1)^2(2a_1)^2(3a_1)^2$ and $(1a_1)^2(2a_1)^2(1b_2)^2)$ in the transition state of the $Be+H_2$ system.

The potential energy surfaces for the model $BeH_2 \rightarrow Be+H_2$ reaction pathway[78] calculated for AP1roG using different orbital optimization schemes are illustrated in Figure 2. The

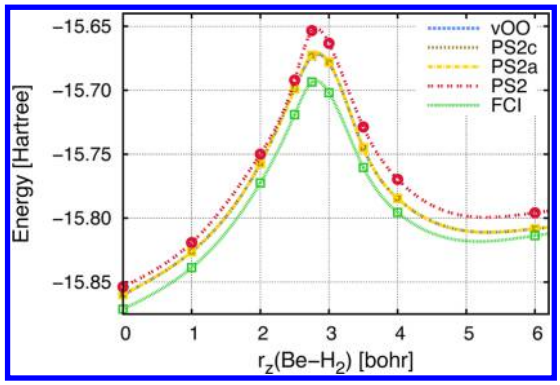


**Figure 2.** Comparison of different orbital optimization techniques of the AP1roG wave function with the FCI reference data for the $BeH_2 \rightarrow Be+H_2$ model reaction.

FCI results are shown for comparison (green line in Figure 2). All variants of orbital optimization lead to a qualitatively correct and smooth potential energy surface along the whole dissociation pathway. The vOO-, PS2c-, and PS2a-AP1roG methods give almost indistinguishable results (differences are much smaller than chemical accuracy, i.e., $\ll 1.5$ m$E_h$) and are close to FCI reference data (cf. Figure 2). The largest deviations from FCI occur in the transition state region ($r_z(x) = 2.75$ bohr), where the multireference character of the


dx.doi.org/10.1021/ct500759q | J. Chem. Theory Comput. 2014, 10, 4873−4882

Be−$H_2$ system is most pronounced.[83] For increasing Be−$H_2$ separations ($r_z \geq 6$ bohr), the differences between FCI and vOO-, PS2c-, and PS2a-AP1roG decrease. In the limiting case $r_z(x) \to \infty$, the system can be described as a composition of a two-electron system (where AP1roG is exact) and a quasi-two-electron system (2 core and 2 valence electrons of the Be atom) where the AP1roG model is a rather good approximation. The performance of the PS2 scheme is slightly worse than vOO-, PS2c-, and PS2a-orbital optimization and the PS2-AP1roG curve deviates strongest from FCI as well as all other orbital optimization techniques. Again, differences are most pronounced around the transition state geometry.

Selected optimized orbitals with large natural occupations numbers are displayed in Figure 3 for three characteristic points

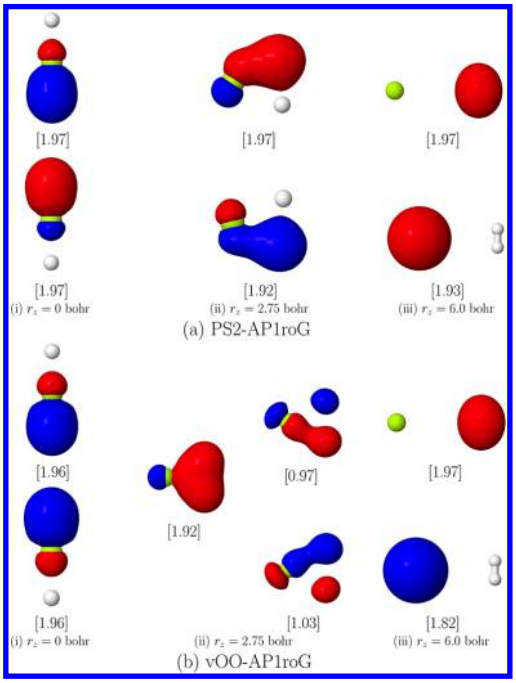


**Figure 3.** Comparison of the $BeH_2$ bonding molecular orbitals. The vOO-, PS2c-, and PS2a-AP1roG optimization techniques yield qualitatively the same molecular orbitals and natural occupation numbers. The natural occupation numbers are determined from the response 1-DM for all orbital sets and are displayed in the square brackets.

along the reaction pathway. AP1roG, like all other wave functions in the APIG family, is a product of natural geminals, and so the 1-electron reduced density matrix—whether computed exactly (which is intractable) or from the energetic response (as is done here)—is diagonal. In general, all orbital optimization schemes yield qualitatively similar, symmetry-broken orbitals. Yet, the PS2 orbital optimization (our most stringent approximation) fails to predict the electronic structure of the transition state correctly (cf. natural occupation numbers in Figure 3). Furthermore, the two highest occupied orbitals are more delocalized compared to the corresponding vOO-, PS2c-, and PS2a-optimized orbitals. We should note that the vOO-, PS2c- and PS2a-AP1roG natural occupation numbers (and the resulting wave functions) fully agree with an MC-SCF (or FCI) description of the transition state structure of Be−$H_2$.[78]

**4.2. The Automerization Process of Cyclobutadiene.** Figure 4 portrays the self-automerization of cyclobutadiene from its stable rectangular geometry, through its transition state

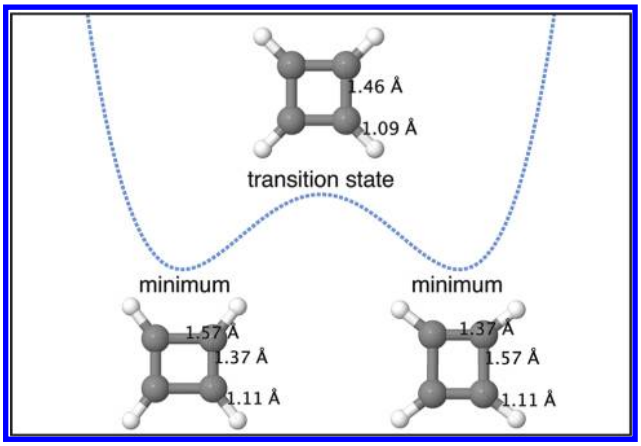


**Figure 4.** Schematic representation of the automerization process of cyclobutadiene.

(with a square geometry) and back to the rectangular structure, rotated by 90°.[88] It is generally accepted that the cyclobutadiene molecule in its transition state structure bears a significant multireference character.[89−94] A reliable theoretical description of the barrier height between the ground and transition state structures requires multireference methods.

Total energies and barrier heights for the automerization process of cyclobutadiene (as shown in Figure 4) obtained from different quantum chemistry methods are collected in Table 2. As shown in Table 2, PS2c- and PS2a-AP1roG total energies are very close to the vOO-AP1roG results. All orbital-optimized AP1roG barrier heights are similar, approximately 20 kcal/mol. Although orbital-optimized AP1roG overestimates the automerization barrier by 10 kcal/mol compared to multireference coupled cluster as well as experiment, it outperforms both CASSCF and NEVPT2, which differ by more than 20 kcal/mol from the Mk-MRCCSD(T) reference.

Selected natural orbitals and the natural occupation numbers of vOO-, PS2c-, and PS2a-AP1roG as well as MP2 and CAS(20,16)SCF are collected in Figure 5. While the vOO-, PS2c-, and PS2a-AP1roG molecular orbitals are localized (symmetry-broken) and bear similar occupation numbers, the PS2-orbital optimization results in delocalized orbitals with natural occupation numbers closer to 2.0 (doubly occupied) and 0.0 (unoccupied) (see Figure 5(b)). However, the absolute differences in occupation numbers between PS2-AP1roG and the other AP1roG orbital optimization techniques are small and amount up to 0.07. In contrast to AP1roG, MP2 predicts smaller natural occupation numbers for "occupied" and larger natural occupation numbers for "unoccupied" molecular orbitals for both the ground and transition state structures of cyclobutadiene. For the ground state, the CASSCF natural occupation numbers are similar to those obtained from AP1roG, while for the transition state structure, the symmetry of the CASSCF $\pi$-orbitals breaks down (similar to the symmetry-broken $\pi$-orbital in Figure 5(a-ii)), leading to two orbitals with natural occupation numbers close to 1.0. This symmetry-breaking lowers the energy of the transition state which artificially decreases the CAS(20,16)SCF barrier height for the automerization reaction.

**4.3. Bicyclic and Monocyclic Forms of the Pyridyne Biradical.** Another multireference model problem is the energetic stability of the 2,6-didehydropyridyne (pyridyne) molecule in its monocyclic and bicyclic forms. The degree of multireference character in these systems strongly depends on


dx.doi.org/10.1021/ct500759q | J. Chem. Theory Comput. 2014, 10, 4873−4882

**Table 2. Barrier Heights of the Automerization Process of Cyclobutadiene**[a]

| | total energy [Hartree] | | barrier height | |
|---|---|---|---|---|
| method | GS | TS | [Hartree] | [kcal/mol] |
| PS2-AP1roG | −153.719 321 | −153.690 619 | 0.028 702 | 18.0 (+10.2) |
| PS2a-AP1roG | −153.884 005 | −153.850 491 | 0.033 514 | 21.0 (+13.2) |
| PS2c-AP1roG | −153.886 993 | −153.854 496 | 0.032 497 | 20.4 (+12.6) |
| vOO-AP1roG | −153.887 097 | −153.854 631 | 0.032 466 | 20.4 (+12.6) |
| MP2 | −153.643 539 | −153.592 092 | 0.051 447 | 32.3 (+24.5) |
| CAS(4,4)SCF | −153.713 999 | −153.630 231 | 0.083 768 | 52.6 (+44.8) |
| NEVPT2/CAS(4,4) | −154.190 998 | −154.125 766 | 0.065 232 | 40.9 (+33.1) |
| CAS(20,16)SCF | −153.814 502 | −153.758 254 | 0.056 248 | 35.3 (+27.5) |
| NEVPT2/CAS(20,16) | −154.167 433 | −154.101 856 | 0.065 577 | 41.2 (+33.4) |
| Mk-MRCCSD(T)[92] | | | | 7.8 |
| experiment[88] | | | | 1.6−10 |

[a]Differences with respect to the multireference Mk-MRCCSD(T) results are given in parentheses. GS: ground state; TS: transition state.

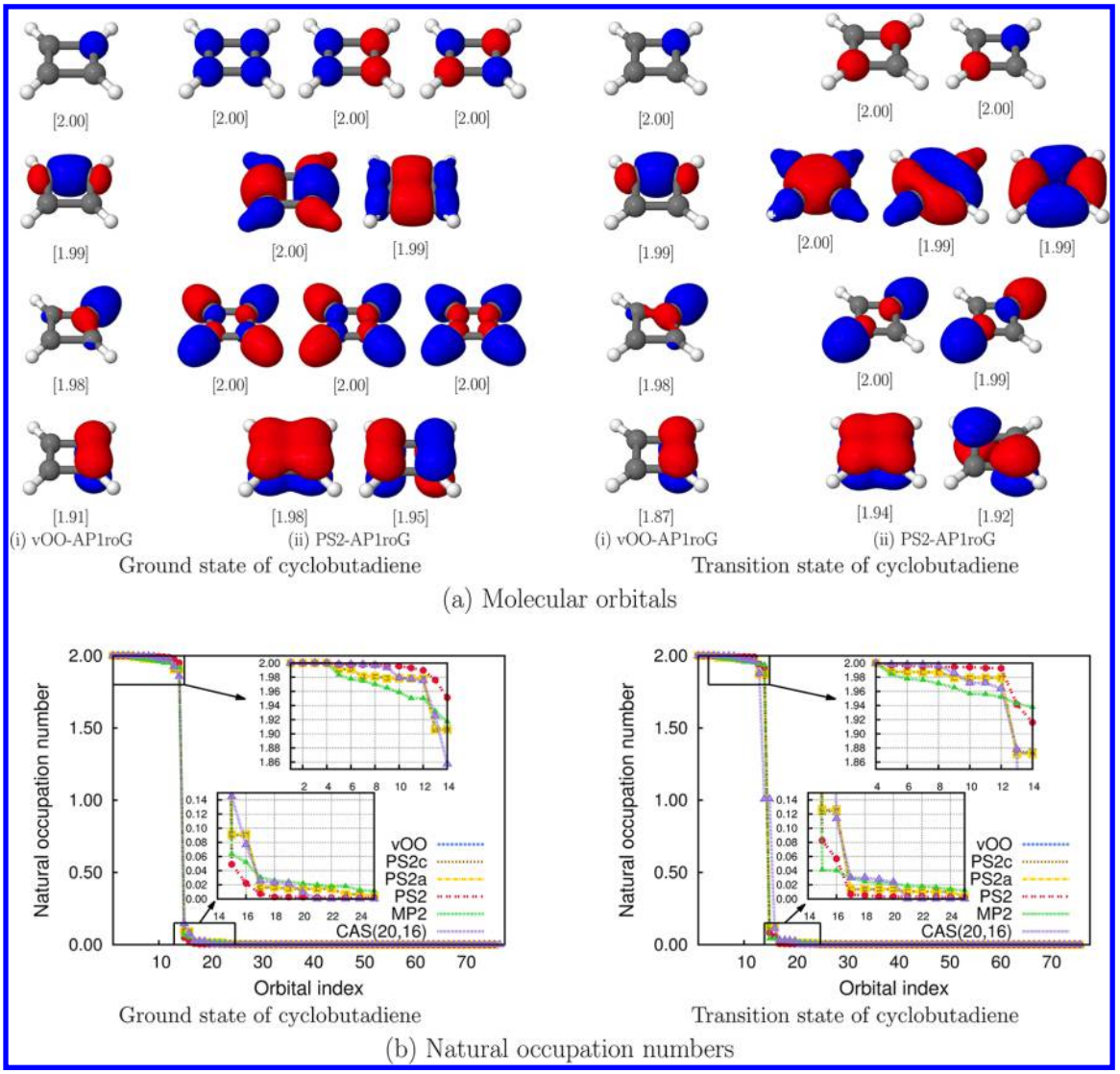


**Figure 5.** (a) Valence occupied vOO- and PS2-AP1roG molecular orbitals for the rectangular and square (transition state) geometries of cyclobutadiene. The vOO-, PS2c-, and PS2a-AP1roG optimization techniques yield qualitatively the same molecular orbitals. (b) vOO-, PS2c-, PS2a-, and PS2-AP1roG natural occupation numbers for the rectangular and square (transition state) structures of cyclobutadiene. The natural occupation numbers are determined from the response 1-DM for all orbital sets and are displayed in the square brackets.

the distance between the two radical centers, which makes it a remarkably challenging system for standard or conventional quantum chemistry methods.[14,73,86,95]

Table 3 summarizes the total energies of the monocyclic and bicyclic forms of pyridyne as well as their relative stability. All AP1roG orbital optimization schemes correctly predict the


dx.doi.org/10.1021/ct500759q | J. Chem. Theory Comput. 2014, 10, 4873−4882

**Table 3. Energetic Stability of the Monocyclic and Bicyclic Forms of the Pyridyne Molecule[b]**

| | total energy [Hartree] | | ΔE(bicyclic,monocyclic) | |
|---|---|---|---|---|
| method[a] | monocyclic | bicyclic | [Hartree] | [kcal/mol] |
| PS2a-AP1roG | −245.806 197 | −245.797 390 | 0.008 807 | 5.5 (−3.3) |
| PS2c-AP1roG | −245.822 958 | −245.798 196 | 0.024 763 | 15.5 (+6.7) |
| vOO-AP1roG | −245.823 951 | −245.799 810 | 0.024 140 | 15.2 (+6.4) |
| MP2 | −246.414 371 | −246.396 546 | 0.017 825 | 11.2 (+2.4) |
| CAS(8,8)SCF | −245.500 591 | −245.467 299 | 0.033 291 | 20.9 (+12.1) |
| NEVPT2/CAS(8,8) | −246.403 581 | −246.393 769 | 0.009 812 | 6.2 (−2.6) |
| CCSD[86] | | | | −3.6 (−12.4) |
| tailored CCSD[14] | | | | 6.8 (−2.0) |
| tailored CCSD(T)[14] | | | | 9.0 (+0.2) |
| Mk-MRCCSD(T)[86] | | | | 8.8 |

[a]In AP1roG, MP2, CASSCF ,and NEVPT2 calculations we used the same geometries as in ref 95. [b]Differences with respect to the Mk-MRCCSD(T) reference value are given in parentheses.

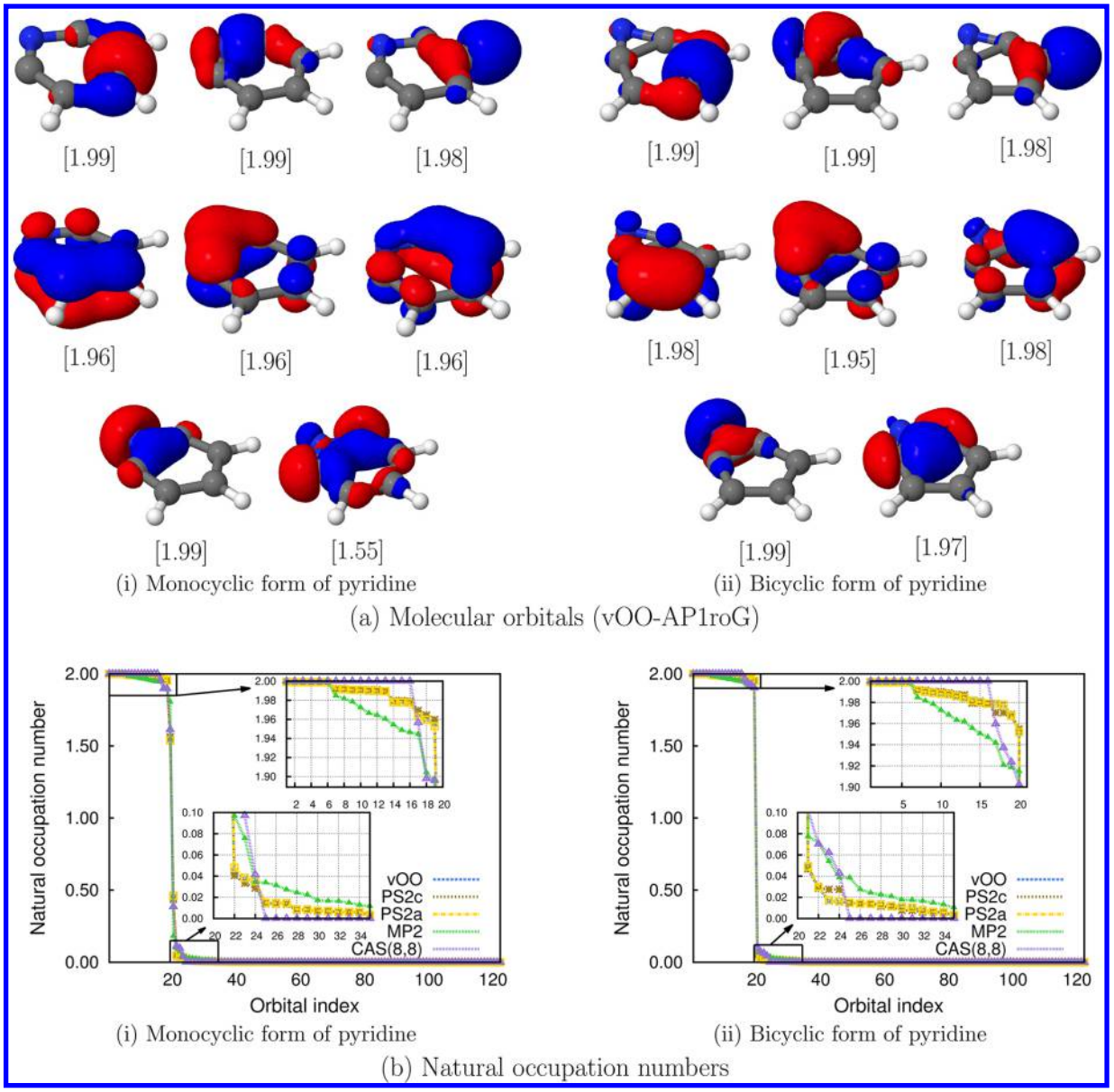


**Figure 6.** (a) Valence occupied vOO-AP1roG molecular orbitals of the monocyclic and bicyclic forms of pyridyne. The vOO-, PS2c-, and PS2a-AP1roG optimization techniques yield qualitatively the same molecular orbitals. (b) vOO-, PS2c-, and PS2a-AP1roG natural occupation numbers for two forms of pyridyne. The natural occupation numbers are determined from the response 1-DM for all orbital sets and are displayed in the square brackets.


dx.doi.org/10.1021/ct500759q | J. Chem. Theory Comput. 2014, 10, 4873−4882

monocyclic form of pyridyne as being the more stable one. We should note that the PS2 results are not shown due to convergence difficulties. Specifically, different initial orbital guesses (delocalized canonical HF, localized vOO-AP1roG, and PS2a-AP1roG) did not promote convergence of PS2-AP1roG. As observed above, vOO- and PS2c-AP1roG yield very similar total energies and energy splittings between the monocyclic and bicyclic forms of pyridyne, approximately 15 kcal/mol. This energy difference is reduced to about 5 kcal/mol for PS2a-AP1roG, in good agreement with NEVPT2 and Mk-MRCCSD-(T) reference data.

Selected vOO-AP1roG molecular orbitals and the natural occupation numbers are displayed in Figure 6. Despite energetic differences, all AP1roG orbital-optimization schemes yield similar, symmetry-broken (localized, partly hybrid), molecular orbitals as well as similar natural occupation numbers. (Differences are much smaller than 0.02.) Note that the CAS(8,8)SCF natural occupation numbers of the active valence molecular orbitals deviate more from the doubly occupied (2.0) and unoccupied (0.0) reference values than the corresponding occupation numbers obtained by any AP1roG orbital optimization scheme.

**4.4. The Delocalized Nature of the Benzene Molecule.** The aromatic stability of benzene has attracted a lot attention from theoretical chemists over the past decade.[96−100] While the lowest energy of the benzene molecule is found in $D_{6h}$ point group geometry where all C−C distances are equally long, approximate methods based on electron pairing (GVB-PP and CC-based PP) and electron localization tend to break this symmetry leading to a $D_{3h}$-symmetric structure.[97,98,100] This issue has been attributed to the localized nature of the three $\pi$- and $\pi^*$-orbitals of benzene, which are constrained to form three partial double bonds in two resonance structures.[98,100]

Since orbital optimized geminal approaches investigated in this work belong to the group of localized methods, we tested to which extent they break the symmetry of benzene. For that reason, we constructed the distortion path of benzene in terms of two rigid (triangular) fragments as described in ref 99. Our starting geometry contains equivalent C−C bonds of 1.40 Å and C−H bonds of 1.09 Å, while the distortion angle ranges from 0.0 to 3.0°.

Figure 7 shows the potential energy surface of the hypothetical distortion pathway obtained from vOO-, PS2c-, and PS2a-AP1roG. We should note that PS2-AP1roG suffered from convergence difficulties for larger distortion angles, and hence the results are not discussed here. As expected, all AP1roG orbital-optimization techniques lead to symmetry-broken solutions and predict the $D_{3h}$-symmetric structure of benzene to be more stable. Apart from small differences in absolute total energies, vOO-AP1roG and PS2c-AP1roG result in almost indistinguishable potential energy surfaces. Both approaches predict an energy minimum for a distortion angle of approximately 1.8°, which is lower by 2.85 kcal/mol from the $D_{6h}$ structure. The symmetry breaking of benzene can be further reduced to 2.25 kcal/mol using the PS2a-AP1roG optimization scheme. We should emphasize that AP1roG (without orbital optimization) does not break the symmetry of benzene for delocalized (Hartree−Fock) molecular orbitals and correctly predicts the $D_{6h}$ structure as the most stable one. Moreover, based on results from ref 69 it seems likely that the $D_{6h}$ structure can be obtained if one considers orbital-pairing models (e.g., unrestricted or generalized AP1roG) that break spin-symmetry. This will be a subject of our future publication.

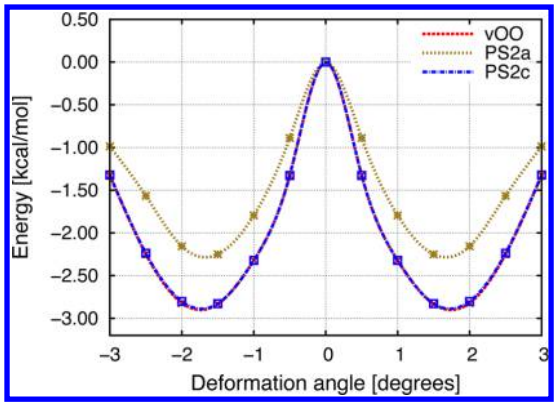


**Figure 7.** Distortion of benzene using different orbital optimization schemes for AP1roG. The absolute reference energies for vOO-, PS2c-, and PS2a-AP1roG are −231.191143, −231.190984, and −231.186464 Hartree, respectively.

## 5. CONCLUSIONS

We have introduced two nonvariational orbital optimization schemes for the AP1roG wave function. These methods can be viewed as refinements of our recently presented projected-seniority-two (PS2) orbital optimization approach.

The accuracy of both methods has been compared to the PS2- and variational orbital-optimized (vOO) techniques for a set of challenging multireference systems. Our studies reveal that the accuracy of PS2a- and PS2c-AP1roG is similar to vOO-AP1roG in most cases. In particular, the PS2c orbital optimization scheme yields total electronic energies and energy splittings that are similar to the variational orbital optimization counterpart. As expected, the PS2a-AP1roG approach gives total electronic energies that are higher than PS2c-AP1roG and vOO-AP1roG, because of additional constraints in the orbital gradient that are not present in PS2c-AP1roG and vOO-AP1roG. For all investigated (multireference) molecules, both PS2a- and PS2c-optimized molecular orbitals are essentially indistinguishable from vOO-AP1roG molecular orbitals. Furthermore, all three orbital optimization methods produce symmetry-broken solutions (localized, hybrid molecular orbitals).

In contrast to PS2c-, PS2a-, and vOO-AP1roG, the PS2 optimization and its convergence behavior are sensitive to the initial guess orbitals. Specifically, we observed that PS2-AP1roG tends to alleviate symmetry-breaking and leads to more delocalized molecular orbitals if localized orbitals are used as initial guess. However, the PS2 orbital optimization scheme suffers from convergence difficulties for larger molecular systems, which can be related to the severe approximations made in the PS2 orbital gradient. By contrast, the convergence of PS2a- and PS2c-AP1roG is more robust. While the PS2 orbital optimization leads to faster and smoother convergence when (delocalized) canonical orbitals are used as initial guess, PS2a-, PS2c-, and vOO-AP1roG converge faster when localized orbitals are provided as starting orbitals.

Although PS2- and PS2a-AP1roG require parts of the three-particle reduced density matrix for the calculation of the orbital gradient, all presented AP1roG orbital-optimization schemes are limited by the four-index transformation of the two-electron repulsion integrals that scales as $O(N^5)$. We should note that a level shift had to be applied to the orbital Hessian in the PS2a-

approach so that smooth convergence could be achieved. This, however, destroys the quadratic convergence. Furthermore, convergence difficulties of all nonvariational orbital optimization schemes might be attributed to our pragmatic assumption of restricting the projection manifold to singly pair excited determinants. This problem could be alleviated by including also higher pair excitations. In practical applications, we, therefore, recommend vOO-AP1roG because of its stable convergence and its robustness against the initial guess orbitals for larger molecular systems (see also ref 61 for additional examples). The nonvariational orbital-optimization techniques, however, can be used to dodge local minima if convergence difficulties are encountered in the variational orbital-optimization scheme.

Finally, our study on multireference problems supports that orbital-optimized AP1roG can be considered as an alternative to standard quantum chemistry methods. For the systems investigated in this work, PS2a-, PS2c-, and vOO-AP1roG approaches provide lower total electronic energies than CASSCF and yield energy splittings that are considerably closer to NEVPT2 or multireference CC reference data. AP1roG has mean-field like scaling and does not require selecting an active space.

## AUTHOR INFORMATION


### Corresponding Authors

*Phone: 905-525-9140, ext. 24162. Fax: 905-522-2509. E-mail: ayers@mcmaster.ca.

*E-mail: bogusl@mcmaster.ca.


### Notes

The authors declare no competing financial interest.

## ACKNOWLEDGMENTS

We gratefully acknowledge financial support from the Natural Sciences and Engineering Research Council of Canada. K.B. acknowledges the financial support from the Swiss National Science Foundation (P2EZP2 148650). P.B. with S.D.B. and D.V.N acknowledge financial support from FWO-Flanders and the Research Council of Ghent University. S.D.B is an FWO postdoctoral fellow. The authors acknowledge support for computational resources from SHARCNET, a partner consortium in the Compute Canada national HPC platform. We had many helpful discussions on geminals with Gustavo E. Scuseria, Paul A. Johnson, and Peter A. Limacher.

## REFERENCES


(1) Szabo, A.; Ostlund, N. S. *Modern Quantum Chemistry: Introduction to Advanced Electronic Structure Theory*; McGraw-Hill: New York, 1989.

(2) Helgaker, T.; Jørgensen, P.; Olsen, J. *Molecular Electronic-Structure Theory*; Wiley: New York, 2000.

(3) Coester, F.; Kümmel, H. *Nucl. Phys.* **1960**, *17*, 477−485.

(4) Bartlett, R. J.; Stanton, J. F. *Rev. Comput. Chem.* **1994**, *5*, 65−169.

(5) Crawford, C. D.; Schaefer III, H. F. *Reviews in Computational Chemistry*; Wiley: New York, 2008; Vol. *14*; p 33.

(6) Bartlett, R. J.; Musiał, M. *Rev. Mod. Phys.* **2007**, *79*, 291−350.

(7) Szalay, P. G.; Müller, T.; Gidofalvi, G.; Lischka, H.; Shepard, R. *Chem. Rev.* **2012**, *112*, 108−81.

(8) Roos, B.; Taylor, P. R. *Chem. Phys.* **1980**, *48*, 157−173.

(9) Werner, H.-J.; Knowles, P. J. *J. Chem. Phys.* **1985**, *82*, 5053−5063.

(10) Olsen, J.; Roos, B. O.; Jørgensen, P.; Jensen, H. J. A. *J. Chem. Phys.* **1988**, *89*, 2185−2192.

(11) Ma, D.; Li Manni, G.; Gagliardi, L. *J. Chem. Phys.* **2011**, *135*, 044128.

(12) Jeziorski, B. *Mol. Phys.* **2010**, *108*, 3043−3054.

(13) Ivanov, V. V.; Lyakh, D. I.; Adamowicz, L. *Phys. Chem. Chem. Phys.* **2009**, *11*, 2355−2370.

(14) Lyakh, D. I.; Musiał, M.; Lotrich, V. F.; Bartlett, R. J. *Chem. Rev.* **2012**, *112*, 182−243.

(15) Nooijen, M.; Demel, O.; Datta, D.; Kong, L.; Shamasundar, K. R.; Lotrich, V.; Huntington, L. M.; Neese, F. *J. Chem. Phys.* **2014**, *140*, 081102.

(16) Cullen, J. *Chem. Phys.* **1996**, *202*, 217−229.

(17) Small, D. W.; Lawler, K. V.; Head-Gordon, M. *J. Chem. Theory Comput.* **2014**, *10*, 2027−2040.

(18) Henderson, T. M.; Dukelsky, J.; Scuseria, G. E.; Signoracci, A.; Duguet, T. *Phys. Rev. C* **2014**, *89*, 054305.

(19) White, S. R. *Phys. Rev. Lett.* **1992**, *69*, 2863−2866.

(20) Schollwöck, U. *Rev. Mod. Phys.* **2005**, *77*, 259−315.

(21) Legeza, O.; Noack, R.; Sólyom, J.; Tincani, L. In *Computational Many-Particle Physics*; Fehske, H., Schneider, R., Weiße, A., Eds.; Lect. Notes Phys.; Springer: Berlin/Heidelerg, 2008; Vol. *739*; pp 653−664.

(22) Chan, G. K.-L.; Sharma, S. *Annu. Rev. Phys. Chem.* **2011**, *62*, 465−481.

(23) Marti, K. H.; Reiher, M. *Phys. Chem. Chem. Phys.* **2011**, *13*, 6750−6759.

(24) Wouters, S.; Van Neck, D. *Eur. Phys. J. D* **2014**, *68*, 272.

(25) Marti, K. H.; Malkin Ondík, I.; Moritz, G.; Reiher, M. *J. Chem. Phys.* **2008**, *128*, 014104.

(26) Boguslawski, K.; Marti, K. H.; Legeza, O.; Reiher, M. *J. Chem. Theory Comput.* **2012**, *8*, 1970−1982.

(27) Boguslawski, K.; Tecmer, P.; Legeza, O.; Reiher, M. *J. Phys. Chem. Lett.* **2012**, *3*, 3129−3135.

(28) Tecmer, P.; Boguslawski, K.; Legeza, O.; Reiher, M. *Phys. Chem. Chem. Phys.* **2014**, *16*, 719−727.

(29) Wouters, S.; Poelmans, W.; Ayers, P. W.; Van Neck, D. *Comput. Phys. Commun.* **2014**, *185*, 1501−1514.

(30) Mottet, M.; Tecmer, P.; Boguslawski, K.; Legeza, O.; Reiher, M. *Phys. Chem. Chem. Phys.* **2014**, *16*, 8872−8880.

(31) Wouters, S.; Bogaerts, T.; Van Der Voort, P.; Van Speybroeck, V.; Van Neck, D. *J. Chem. Phys.* **2014**, *140*, 241103.

(32) Duperrouzel, C.; Tecmer, P.; Boguslawski, K.; Barcza, G.; Legeza, O.; Ayers, P. *Chem. Phys. Lett.* **2014**, arXiv preprint arXiv:1409.4867v1.

(33) Jiménez-Hoyos, C. A.; Henderson, T. M.; Tsuchimochi, T.; Scuseria, G. E. *J. Chem. Phys.* **2012**, *136*, 164109.

(34) Jiménez-Hoyos, C. A.; Rodrguez-Guzmán, R.; Scuseria, G. E. *J. Chem. Phys.* **2013**, *139*, 224110.

(35) Surján, P. R. *Correlation And Localization*; Springer: Berlin, 1999; pp 63−88.

(36) Surján, P. R.; Szabados, A.; Jeszenszki, P.; Zoboki, T. *J. Math. Chem.* **2012**, *50*, 534−551.

(37) Hurley, A. C.; Lennard-Jones, J.; Pople, J. A. *Proc. R. Soc. London, Ser. A* **1953**, *220*, 446−455.

(38) Goddard, W. A.; Amos, A. *Chem. Phys. Lett.* **1972**, *13*, 30−35.

(39) Goddard, W. A.; Dunning, T. H., Jr.; Hunt, W. J.; Hay, P. J. *Acc. Chem. Res.* **1973**, *6*, 368−376.

(40) Parr, R. G.; Ellison, F. O.; Lykos, P. G. *J. Chem. Phys.* **1956**, *24*, 1106−1107.

(41) Parks, J. M.; Parr, R. G. *J. Chem. Phys.* **1958**, *28*, 335−345.

(42) Kutzelnigg, W. *J. Chem. Phys.* **1964**, *40*, 3640−2647.

(43) Kutzelnigg, W. *Theor. Chim. Acta* **1965**, *3*, 241−253.

(44) Rassolov, V. A. *J. Chem. Phys.* **2002**, *117*, 5978.

(45) Coleman, A. J. *J. Math. Phys.* **1965**, *6*, 1425−1431.

(46) Bratoz, S.; Durand, P. *J. Chem. Phys.* **1965**, *43*, 2670−2679.

(47) Silver, D. M. *J. Chem. Phys.* **1969**, *50*, 5108−5116.

(48) Silver, D. M. *J. Chem. Phys.* **1970**, *52*, 299−303.

(49) Náray-Szabó, G. *J. Chem. Phys.* **1973**, *58*, 1775−1776.

(50) Náray-Szabó, G. *Int. J. Qunatum Chem.* **1975**, *9*, 9−21.

(51) Surján, P. R. *Phys. Rev. A* **1984**, *30*, 43−50.

(52) Surján, P. R. *Phys. Rev. A* **1985**, *32*, 748−755.

(53) Surján, P. R. *Int. J. Quantum Chem.* **1994**, *52*, 563−574.

(54) Surján, P. R. *Int. J. Quantum Chem.* **1995**, *55*, 109−116.

(55) Rosta, E.; Surján, P. R. *Int. J. Quantum Chem.* **2000**, *80*, 96−104.
(56) Rosta, E.; Surján, P. R. *J. Chem. Phys.* **2002**, *116*, 878−889.
(57) Limacher, P. A.; Ayers, P. W.; Johnson, P. A.; De Baerdemacker, S.; Van Neck, D.; Bultinck, P. *J. Chem. Theory Comput.* **2013**, *9*, 1394−1401.
(58) Johnson, P. A.; Ayers, P. W.; Limacher, P. A.; De Baerdemacker, S.; Van Neck, D.; Bultinck, P. *Comput. Chem. Theory* **2013**, *1003*, 101−113.
(59) Boguslawski, K.; Tecmer, P.; Ayers, P. W.; Bultinck, P.; De Baerdemacker, S.; Van Neck, D. *Phys. Rev. B* **2014**, *89*, 201106(R).
(60) Scuseria, G. E.; Schaefer, H. F., III *Chem. Phys. Lett.* **1987**, *142*, 354−358.
(61) Boguslawski, K.; Tecmer, P.; Limacher, P. A.; Johnson, P. A.; Ayers, P. W.; Bultinck, P.; De Baerdemacker, S.; Van Neck, D. *J. Chem. Phys.* **2014**, *140*, 214114.
(62) Talmi, I. *Simple models of complex nuclei*; CRC Press: Chur, 1993; Vol. *7*.
(63) Bytautas, L.; Henderson, T. M.; Jiménez-Hoyos, C. A.; Ellis, J. K.; Scuseria, G. E. *J. Chem. Phys.* **2011**, *135*, 044119.
(64) Alcoba, D. R.; Torre, A.; Lain, L.; Massaccesi, G. E.; Ona, O. B. *J. Chem. Phys.* **2013**, *139*, 084103.
(65) Alcoba, D. R.; Torre, A.; Lain, L.; Massaccesi, G. E.; Ona, O. B. *J. Chem. Phys.* **2014**, *140*, 234103.
(66) Pian, J.; Sharma, C. S. *J. Phys. A: Math. Gen.* **1981**, *14*, 1261−1270.
(67) Levy, B.; Berthier, G. *Int. J. Quantum Chem.* **1968**, *11*, 307−319.
(68) Chang, T. C.; Schwarz, W. H. E. *Theor. Chim. Acta* **1977**, *44*, 45−59.
(69) Limacher, P. A.; Kim, T. D.; Ayers, P. W.; Johnson, P. A.; De Baerdemacker, S.; Van Neck, D.; Bultinck, P. *Mol. Phys.* **2014**, *112*, 853−862.
(70) Tecmer, P.; Boguslawski, K.; Limacher, P. A.; Johnson, P. A.; Chan, M.; Verstraelen, T.; Ayers, P. W. *J. Phys. Chem. A* **2014**, DOI: 10.1021/jp502127v.
(71) Stein, T.; Henderson, T. M.; Scuseria, G. E. *J. Chem. Phys.* **2014**, *140*, 214113.
(72) Aidas, K.; Angeli, C.; Bak, K. L.; Bakken, V.; Bast, R.; Boman, L.; Christiansen, O.; Cimiraglia, R.; Coriani, S.; Dahle, P.; et al. *WIREs Comput. Mol. Sci.* **2013**, *4*, 269−284.
(73) Cramer, C. J.; Debbert, S. *Chem. Phys. Lett.* **1998**, *287*, 320−326.
(74) *Horton*, developer version 1.2, written by Verstraelen, T.; Vandenrbande, S.; Chan, M.; Zadeh, F. H.; Gonzalez, C.; Boguslawski, K.; Tecmer, P.; Limacher, P. A.; Malek, A. Ghent (Belgium) and Hamilton (Canada), 2013. http://theochem.github.com/horton/ (accessed April 10, 2014).
(75) Dunning, T. H. *J. Chem. Phys.* **1989**, *90*, 1007−1023.
(76) Feller, D. *J. Comput. Chem.* **1996**, *17*, 1571−1586.
(77) Didier, K.; Elsethagen, B.; T. Sun, L. G.; Chase, V.; Li, J.; Windus, T. L. *J. Chem. Inf. Model.* **2007**, *47*, 1045−1052.
(78) Purvis, G. D.; Shepard, R.; Brown, F. B.; Bartlett, R. J. *Int. J. Quantum Chem.* **1983**, *XXIII*, 835−845.
(79) Hinze, J.; Friedrich, O.; Sundermann, A. *Mol. Phys.* **1999**, *96*, 711−718.
(80) Mahapatra, U. S.; Datta, B.; Mukherjee, D. *J. Chem. Phys.* **1999**, *110*, 6171−6188.
(81) Kallay, M.; Szalay, P. G.; Surjan, P. R. *J. Chem. Phys.* **2002**, *117*, 980−990.
(82) Ruttink, P. J. A.; Van Lenthe, J. H.; Todorov, P. *Mol. Phys.* **2005**, *103*, 2497−2506.
(83) Evangelista, F. A.; Allen, W. D.; Schaefer, H. F. *J. Chem. Phys.* **2006**, *125*, 154113.
(84) Koput, J.; Peterson, K. A. *J. Chem. Phys.* **2006**, *125*, 44306.
(85) Li, H.; Le Roy, R. J. *J. Chem. Phys.* **2006**, *125*, 44307.
(86) Evangelista, F. A.; Prochnow, E.; Gauss, J.; Schaefer, H. F., III *J. Chem. Phys.* **2010**, *132*, 074107.
(87) Gidofalvi, G.; Brozell, S. R.; Shepard, R. *Theor. Chem. Acc.* **2014**, *133*, 1−12.
(88) Whitman, D. W.; Carpenter, B. K. *J. Am. Chem. Soc.* **1982**, *104*, 6473−6474.
(89) Balkova, A.; Bartlett, R. J. *J. Chem. Phys.* **1994**, *101*, 8972−8987.
(90) Eckert-Maksić, M.; Vazdar, M.; Barbatti, M.; Lischka, H.; Maksić, Z. B. *J. Chem. Phys.* **2006**, *125*, 64310.
(91) Demel, O.; Shamasundar, K. R.; Kong, L.; Nooijen, M. *J. Phys. Chem. A* **2008**, *112*, 11895−11902.
(92) Bhaskaran-Nair, K.; Demel, O.; Pittner, J. *J. Chem. Phys.* **2008**, *129*, 184105.
(93) Li, X.; Paldus, J. *J. Chem. Phys.* **2009**, *131*, 114103.
(94) Lyakh, D. I.; Lotrich, V. F.; Bartlett, R. J. *Chem. Phys. Lett.* **2011**, *501*, 166−171.
(95) Prochnow, E.; Evangelista, F. A.; Schaefer, H. F., III; Allen, W. D.; Gauss, J. *J. Chem. Phys.* **2009**, *131*, 064109.
(96) Cyrański, M. K. *Chem. Rev.* **2005**, *105*, 3773−811.
(97) Hiberty, P. C.; Shaik, S. S.; Lefour, J.-M.; Ohanessian, G. *J. Org. Chem.* **1985**, *50*, 4657−4659.
(98) Shaik, S. S.; Hiberty, P. C. *J. Am. Chem. Soc.* **1985**, *107*, 3089−3095.
(99) Pierrefixe, S. C. A. H.; Bickelhaupt, F. M. *J. Phys. Chem. A* **2008**, *112*, 12816−12822.
(100) Lawler, K. V.; Beran, G. J. O.; Head-Gordon, M. *J. Chem. Phys.* **2008**, *128*, 024107.